High Temperature Material Processes 20(3), 267–278 (2016)

HIGH-ENTROPY TITANIUM–ALUMINUM DIFFUSION COATINGS ON NICKEL ALLOY

V. G. Khyzhniak,[1] T. V. Loskutova,[1] O. E. Datsyuk,[1] I. S. Pohrebova,[1] N. A. Kharchenko,[2] T. P. Hovorun,[2,] A. I. Dehula,[2] I. Ya. Smokovich,[3] & Ya. O. Kravchenko[2]*

[1]*National Technical University of Ukraine "Igor Sikorsky Kyiv Polytechnic Institute," Kyiv, 03056, Ukraine*

[2]*Sumy State University, Sumy, 40007, Ukraine*

[3]*Otto-von-Guericke University Magdeburg, Magdeburg, 39106, Germany*

[*]Address all correspondence to: T. P. Hovorun, E-mail: tatgovorun@gmail.com

This article describes the new results of the study of the effect of high-entropy titanium–aluminum coating on the structure, microhardness, and heat resistance of nickel alloys. There are presented coatings after three different regimes of the chemical-thermal treatment. The obtained coatings were characterized by means of scanning electron microscope (SEM) and X-ray diffraction (XRD) analyses.

KEY WORDS: *high-entropy coatings, titanium–aluminum diffusion coatings, chemical-thermal treatment, microhardness, heat resistance, nickel alloys*

1. INTRODUCTION

The requirements of the modern industry have caused the appearance of a new class of materials — so-called high-entropy alloys (HEAs) that combine excellent mechanical properties, thermal stability, and corrosion resistance (Pogrebnyak et al., 2014; Zhang and Zhou, 2007; Krause-Rehberg et al., 2013). These alloys contain at least five metals, and the main feature consists of a phase composition of the solid solution based on the face-centered cubic (fcc) or body-centered cubic (bcc) crystal structures.

In (Pogrebnyak et al., 2014; Zhang and Zhou, 2007; Gorban et al., 2015; Karpets et al., 2015) the correlation between the structure characteristics and the way of production of high-entropy alloys is presented. Among the most common methods of production are casting and mechanical alloying (Pogrebnyak et al., 2014). Moreover, other methods are known: laser cladding of $Al_2CrFeNiCoCuTi_x$, $Al_2CrFeCoCuTiNi_x$, and AlCoCrCuFeNi; selective laser welding of ZrTiVCrFeNi, and thermal spraying

1093-3611/16/$35.00

of $Ni_xCo_{0.6}Fe_{0.2}Cr_ySi_zAlTi_{0.2}$. HEAs produced by laser cladding are characterized by the presence of the cladding zone, heat-affected and bounding zones in their structure. The cladding zone consists of Laves' phases, as well as contains bcc and fcc structures. The bounding zone is actually a transition zone, which contacts from the side of the substrate with the heat affected zone.

The investigations of the properties of some types of coatings based on HEAs, their carbides and nitrides, are presented in Pogrebnyak et al. (2014, 2016a,b); Gorban et al. (2015); Braic et al. (2012); and Tsai et al. (2010). In Gorban et al. (2015) it is demonstrated that during a magnetron sputtering of TiZrVNbTa, AlCrFeCoNiCuV, and TiZrHfNbTaCr alloys, the coatings of different phase composition with a hardness of 10.0-19.0 GPa and elastic modulus of 106.0-192.0 GPa are formed.

The review (Pogrebnyak et al., 2014) considers a large number of works devoted to the practical use of HEAs: nuclear power engineering, energy engineering, tools manufacture, etc. It is expected that HEA-based coatings will have a high heat resistance and thus improve the performance properties of refractory alloys. The scientific and technical information regarding the production of diffusion coatings on the basis of high-entropy alloys is limited. In the present work, a method of a diffusion metallization for creation of HEAs coatings is presented (Voroshnin et al., 2010).

The aim of this work is to establish the possibility of HEAs coatings production on the surface of a nickel alloy by involving elements of the substrate (Ni, Cr, W, Mo, Ti, Co, Al) and saturating elements (Ti, Al), to determine the composition and structure of the obtained coatings after different regimes of chemical-thermal treatment.

2. MATERIALS AND METHODS

As an object of research a superalloy on NiCrCoTiAlWMo the nickel base: Cr (14.8%), Co (10.6%), Ti (4.5%), Al (0.7%), W (5.2%), and Mo (2.1%) was selected. This alloy belongs to a class of deformed alloys produced at high temperatures. The typical thermal treatment consists of two steps of hardening: the first one from 1200 to 1210°C for 4 h of holding; the second — from 1050°C with 4 h of holding; cooling in air; aging at 850°C for 8 h (Kolomytsev, 1991). Technologically it is predominant to carry out chemical-thermal treatment at a second hardening temperature of 1050^oC. The cooling after titanium–aluminum saturation was conducted with speeds of 25–30°C/min and 10–15°C/min.

The saturation with titanium and aluminum was performed in the mixture of powders: Ti (50 wt.%), Al (10 wt.%), Al_2O_3 (35 wt.%), and NH_4Cl (5 wt.%) in a consumable storage container at 1050°C for 4 h. Some amount of samples was subjected to preliminary nitriding by physical vapor deposition. The nitride layer (Ti, Zr)N of thickness 5.5–6.0 μm was used as a barrier. The X-ray diffraction patterns were produced with a DRON-3M diffractometer in monochromatic Cu-K_α radiation, to identify the phase composition; the Powder Cell 2.2 software package

was applied. A layer by layer analysis was made by mechanical grinding of the specimen's surface on diamond discs. The thickness of the removed diffusion zone was about 15 μm.

The chemical composition of the coatings was examined by electron microprobe analysis with a CamScan 4D electron scanning microscope and an INCA-200 energy analyzer, an error of the measurement is ±0.3%. Microstructural studies were carried out on a CamScan 4D electron microscope after etching the samples with a Murakami reagent, followed by 3.0% solution of nitric acid in ethanol. The microhardness measurement and the specification of the coating thickness were determined with a PMT-3 meter, no less than in 20 fields of view.

3. RESULTS AND DISCUSSION

Depending on the speed of cooling after titanium–aluminum metallization and the initial surface conditions, samples were obtained after three different regimes of chemical-thermal treatments (the saturation mixture preserved its composition, as well as temperature–time conditions were preserved at 1050°C, for 4 h):

1) titanium–aluminum saturation; cooling rate at 10–15°C/min;
2) titanium–aluminum saturation; cooling rate at 25–30°C/min;
3) titanium–aluminum saturation of the samples with a preliminary nitride layer (Ti, Zr)N; cooling rate at 10–15°C/min.

The results of the phase and chemical composition, structure examinations of the coatings obtained on nickel superalloy are shown in Figs. 1 and 2 and Tables 1 and 2. It is established that titanium–aluminum metallization leads to the formations of multiphase and multilayer coatings characterized by the presence of cladding and bounding zones. According to the results presented, the samples produced by regimes 1 and 3 differ in the structure, phase compositions, and in the distribution of chemical elements over the thickness of the coatings.

The feature of the coating structure obtained by regimes 1 and 2 is the presence of an outside zone of oxides in a multilayer: Al_2O_3, Ni_2Ti_4O, and Me_3Ni_3O (where Me is Ti or Al) and an oxynitride zone Ti(N, O), Fig. 1, zone I. The total thickness of the layer is 5.0–8.5 μm. The concentrations of chemical elements in this zone is as follows: Ti 48.0–52.5 wt.% and Al 10.0–18.2 wt.%. Among the elements of the substrate, the largest content is that of nickel: 20.5–31.6 wt.%; the concentrations of cobalt and chromium are 2.5 and 1.5 wt.%, respectively.

The absence of oxides in the coatings, produced by regime 3, besides the Al_2O_3 layer, is caused by the influence of the barrier layer (Ti, Zr)N, as well as by the conditions of formation of titanium–aluminum coatings. It is clear that the barrier layer inhibits nickel supply from the substrate to the surface, and thus contributes to the occurrence of titanium- and aluminum-rich phases, reducing the ability of the appearance of oxides. The layer with a high titanium and aluminum content is situated

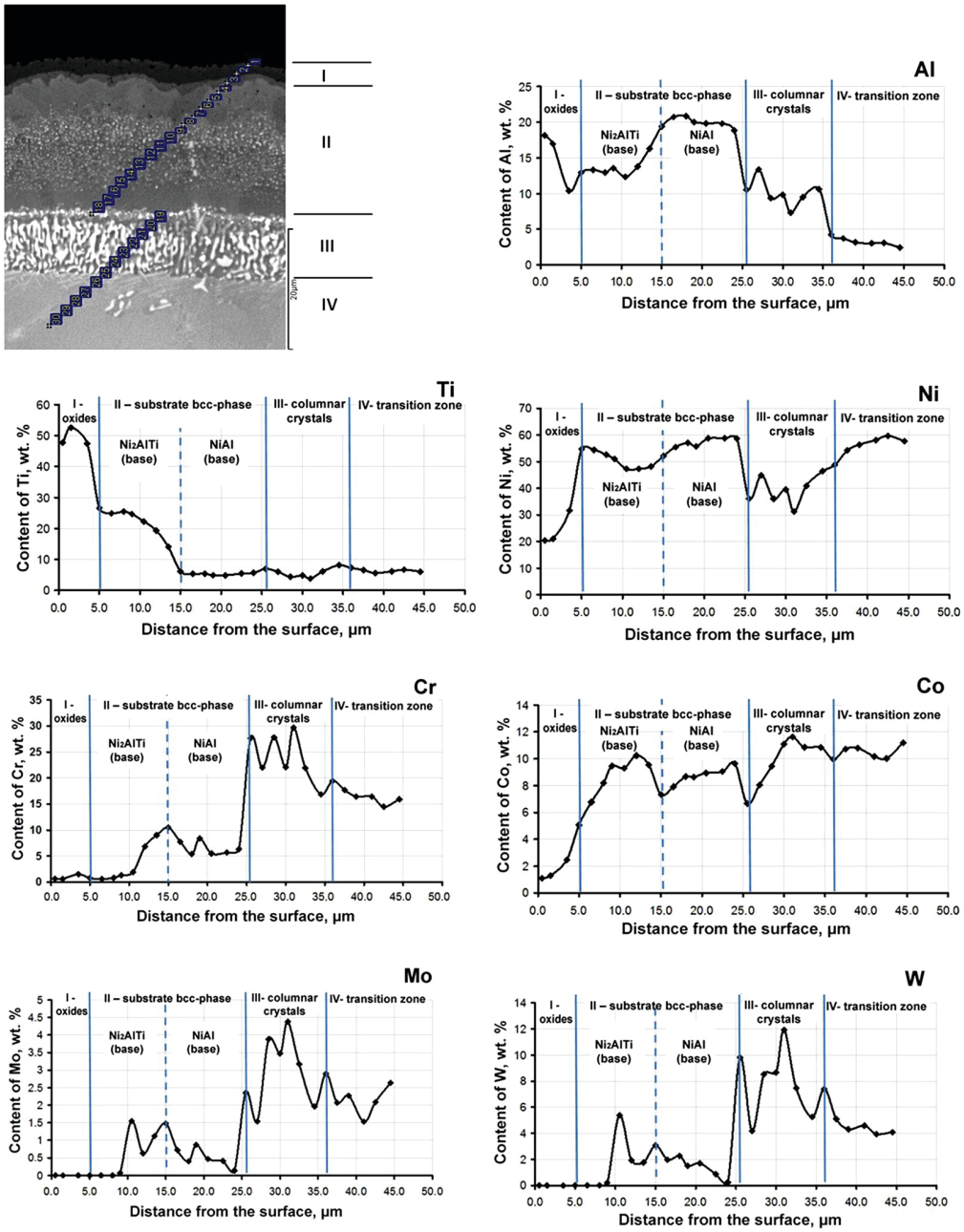

FIG. 1: Distribution of chemical elements over the thickness of titanium–aluminum coatings on the NiCrCoTiAlWMo alloy; regime 1

on the outside of the coatings, and corresponds to the compound $Ni_{0.2}Al_{0.4}Ti_{0.4}$ (a = 0.5011; c = 0.8079 nm).

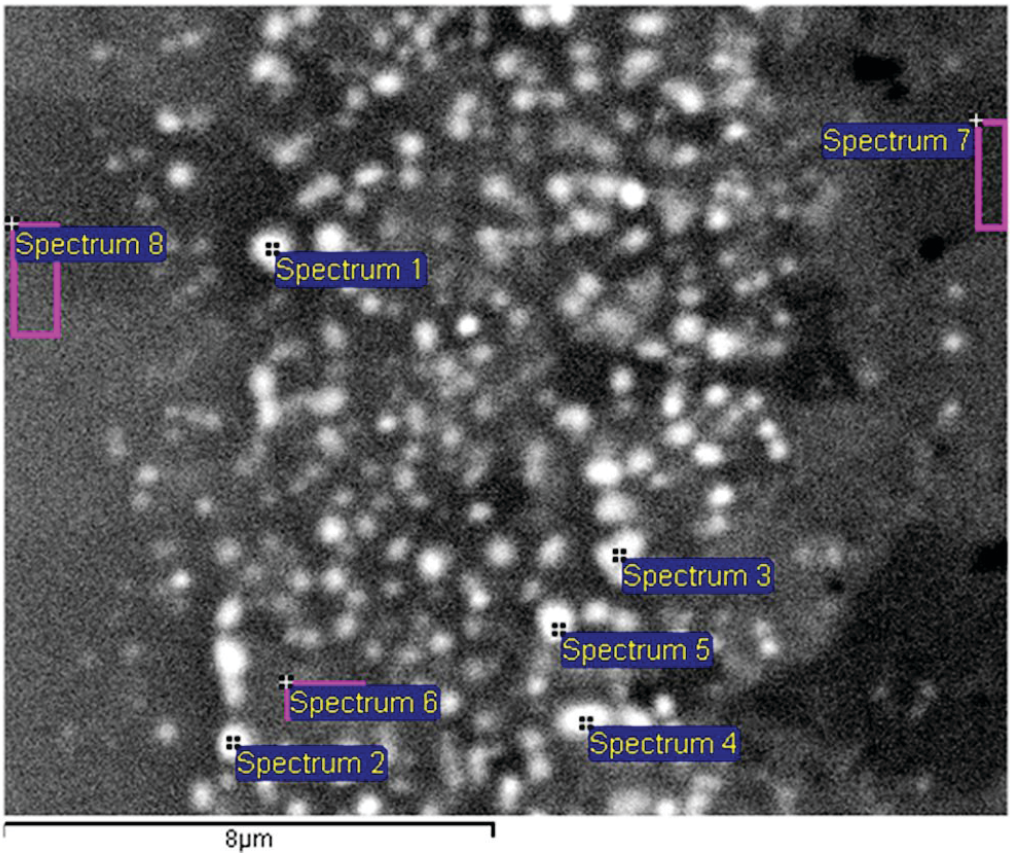

FIG. 2: Microstructure of titanium–aluminum coatings on the NiCrCoTiAlWMo alloy (electron microscope); regime 1, zone II

This compound, which is also known as $Ti(Ti_yNi_xAl_{(1-x-y)})$, is seen on the phase diagram Al–Ti–Ni and is denoted as the λ-phase (Klopotov et al., 2013; Schuster et al., 2007). The thickness of $Ni_{0.2}Al_{0.4}Ti_{0.4}$ layer is 9.5–10.5 μm. It should be mentioned that the concentration of aluminum through the whole layer remains at 18.8–24.4 wt.%.

Zone I in the coatings of regimes 1 and 2 is microstructurally defined as a light or dark-gray streaks. The individual layers of oxides have clear boundaries as almost straight lines and the advanced boundary with zone II, which caused a different thickness of the oxide layer.

Zone II is dark-gray in color with some light impurities of a separate phase in the central part of the coatings (regime 1, Fig. 1, Table 2). The size of the light impurities does not exceed 0.6–0.8 μm. The maximum content of impurities was found in the center of zone II — 25.0–28.0%. Light compounds have the following atomic composition: $Ni_{24}Cr_{36}Al_{16}Co_4Ti_{10}Mo_5W_5$. The dark-gray matrix, where the impuri-

TABLE 1: Phase composition and characteristics of titanium–aluminum* coatings on the NiCrCoTiAlWMo alloy

Regime	Coatings	Phase Composition**	Lattice Parameter, nm	Thickness, μm	Microhardness, GPa
Titanium–aluminum metallization (regime 1)	Cladding zone	I. Oxides: Ti_4Ni_2O Me_3Ni_3O Ti(N,O)	a = 1.1371 a = 1.1248 a = 0.4220	1.5–2.0 2.0–4.0 2.0–4.5	6.6–6.8
		II. Heterogeneous zone dark substrate (external): $Ni_{42}Al_{24}Ti_{26}Cr_1Co_5$; light crystals (external): $Ni_{38}Al_{20}Ti_{14}Cr_9Co_8Mo_5W_6$ dark substrate (internal): $Ni_{48}Al_{35}Ti_5Cr_5Co_6W_{0.5}Mo_5$ light crystals (internal): $Ni_{39}Al_{21}Ti_{10}Cr_{20}Co_7Mo_1W_2$	0.2943 0.2896	22.0–24.0	19.3 10.9
		III. Heterogeneous zone (column structure) light crystals: $Ni_{25}Cr_{40}Co_{10}Mo_{10}W_{15}$; dark crystals: $Ni_{45}Cr_{35}Al_8Co_8W_4$	–	11.0–12.0	2.4–15.3
	Bounding zone	IV –	–	8.0–10.0	4.6–3.0
Titanium–aluminum saturation the samples with a preliminary nitride layer (Ti, Zr)N (regime 3)	Cladding zone	I. Homogeneous zone $Ni_{20}Al_{35}Ti_{38}Cr_{3.0}Co_{4.0}$	a = 0.5007 c = 0.8070	9.5–10.0	6.2–6.8
		II. Heterogeneous zone dark substrate: $Ni_{42}Al_{27}Ti_{21}Co_8Cr_2$ light crystals	0.2956	9.0–12.0	12.0
		(Ti, Zr)N	0.4330	4.5–5.0	22.1
		dark substrate: $Ni_{40}Al_{22}Co_8Ti_{18}Cr_{10}Mo_1W_1$; light crystals: $Ni_{22}Al_5Co_{12}Ti_7Cr_{26}Mo_8W_{20}$	0.2940 –	6.0–12.0	3.2–4.6
		III. Heterogeneous zone (column structure) light crystals: the main elements: Ni, Cr, Co, W;	–	6.0–8.0	3.2–6.2

TABLE 1: *(continued)*

Regime	Coatings	Phase Composition**	Lattice Parameter, nm	Thick-ness, μm	Micro-hardness, GPa
Titanium–alumi-num saturation the samples with a preliminary nitride layer (Ti, Zr)N (regime 3)	Cladding zone	dark crystals: the main elements: Ni, Cr, Co	–	6.0–8.0	3.2–6.2
	Bound-ing zone	IV –	–	5.0–10.0	4.0–3.0

*Titanium–aluminum saturation at 1050°C for 4 h; cooling rate 10–15°C/min.

**Phase and structural components of the coating are located from the surface to the substrate; on the outside there is a layer of Al_2O_3

TABLE 2: Chemical composition of individual components of titanium–aluminum coatings on the NiCrCoTiAlWMo alloy; regime 1, zone II

Spectrum no.	Element Content, wt.%						
	Al	Ti	Cr	Co	Ni	Mo	W
Spectrum 1	12.29	4.08	27.92	6.28	39.93	2.20	7.29
Spectrum 2	15.83	5.24	11.74	7.68	52.91	1.36	5.25
Spectrum 3	11.19	15.72	13.17	10.30	43.86	1.57	4.20
Spectrum 4	8.02	10.35	30.95	6.94	30.46	3.47	9.81
Spectrum 5	8.15	8.59	30.39	6.47	31.24	4.13	11.03
Spectrum 6	20.70	8.64	13.77	8.19	48.71	–	–
Spectrum 7	12.44	24.82	5.74	8.19	48.81	–	–
Spectrum 8	17.28	5.71	5.96	9.38	61.67	–	–

ties are distributed, corresponds to the phase with a bcc lattice (a = 0.2943 nm). The other part of the coating with titanium concentration of about 5.0 wt.% corresponds to a compound with a smaller period of a lattice (a = 0.2896 nm). The difference between the known lattice period of the stoichiometric composition of phase NiAl (a = 0.2887 nm) (Kolomytsev, 1991) and the one defined in the work is caused by the presence of titanium, chromium, and cobalt dissolved in its structure (Fig. 2, Table 2).

It should be noted that molybdenum and tungsten are not included into the dark-phase matrix. A similar relation between element's distributions was identified in the zone of columnar crystals. The number of elements, participating in the high-entropy alloys formation, rises to nine. They are iron, whose content in the center and outside the columnar crystal's zone does not exceed 0.5 wt.%, and rhenium. When the con-

centration of rhenium in the transition zone is 0.8 wt.%, its content in the light columnar crystals zone is 1.5 wt.%. Under the layer of columnar crystals, another zone of light-gray columnar crystals is located on the dark-gray background. The columnar crystals of this zone are mostly a continuation of the previous columnar crystals. In some cases, the areas of the mentioned structure are located at a distance from the coating layer, Fig. 1. The light-gray columnar crystals contain mostly Ni, Cr, Co, and W in the amount 44.5 wt.%, 21.5 wt.%, 11.0 wt.%, and 11.0 wt.%, respectively.

The structure of zone II in the coatings of regime 2 corresponds to the coatings structure produced by regime 1. The coatings of regime 2 differ in size and composition from the multicomponent light compounds in zone II. The compounds are formed in the light-gray substrate of the high-entropy phase (a = 0.2939 nm). The light impurities in the center of zone II have the following atomic composition: $Ni_{24}Cr_{36}Al_{16}Co_4Ti_{10}Mo_5W_5$. This phase is also a bit alloyed by titanium. At the same time, the light impurities on the outside of the diffusion zone have the composition: $Ti_{45}W_{25}Mo_7Ni_6Al_4Cr_7Co_2$, where titanium is a basic element.

The structure of zone II in the coatings of regime 2 (Fig. 3) corresponds to the coatings structure produced by regime 1.

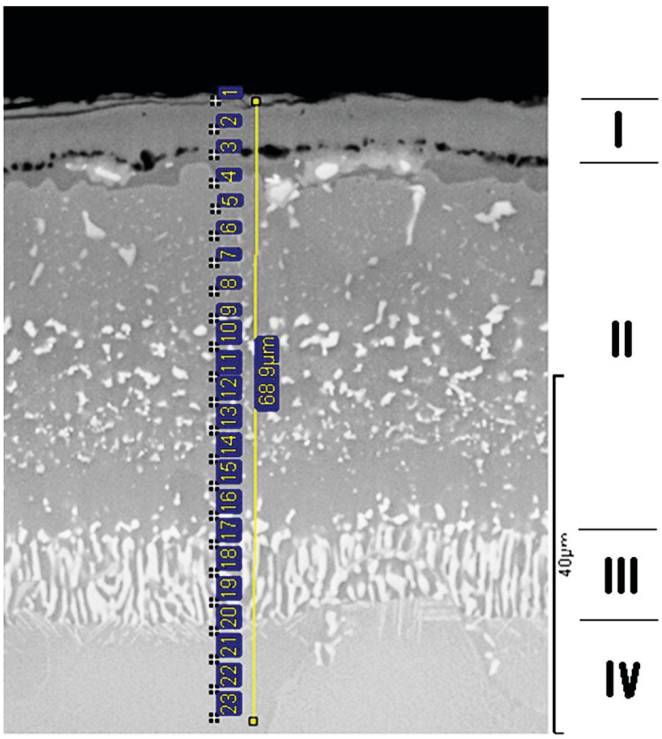

FIG. 3: Microstructure of titanium–aluminum coatings on the NiCrCoTiAlWMo alloy (electron microscope), regime 2

The coatings of regime 2 differ in size and compositon from the multicomponent light compounds in zone II (Fig. 3). The compounds are formed in the light-gray substrate of the high-entropy phase (a = 0.2939 nm). The light impurities in the center of zone II have the following atomic composition: $Ni_{24}Cr_{36}Al_{16}Co_4Ti_{10}Mo_5W_5$. This phase is also a bit alloyed by titanium. At the same time, the light impurities on the outside of the diffusion zone have the composition: $Ti_{45}W_{25}Mo_7Ni_6Al_4Cr_7Co_2$, where titanium is a basic element.

The rate of cooling of samples after titanium–aluminum saturation in regime 2 is almost two times lower than in regimes 1 and 3. It is believed that a relatively higher rate of cooling promotes the formation of a fine structure in zone II, suppressesing the excretion of the titanium-based multicompounds in the diffusion zone.

The barrier layer (Ti, Zr)N in the original alloy slightly slows down the extraction of elements from the substrate to the surface, as well as the diffusion of saturation elements in the alloy during the titanium–aluminum metallization (Khizhnyak and Arshuk, 2011). The thickness of coatings in regimes 1 and 3 is practically identical. The titanium–aluminum saturation of regime 3 is accompanied by the appearance of $Ni_{0.2}Al_{0.4}Ti_{0.4}$ compound on the outside layer (Fig. 4, zone I).

The main constituent of zone II is the layer of the phase with a bcc lattice (a = 0.2956 nm), on the gray background of which the golden-yellow line of (Ti, Zr)N phase with a 5.0–5.5 μm thickness is distinguished, and almost white impurities of different shapes: round shape with a diameter of 5.0–8.5 μm, elongated in a rectangular form 10.0 × 1.0–1.5 μm, etc. The atomic constituents of this compound correspond to $Ni_{22}Cr_{27}W_{20}Al_5Co_{12}Ti_7Mo_7$. The impurities of this phase are mainly situated in front of the (Ti, Zr)N layer. In the publications (Maboyadzhan et al., 2008; Klopotov et al., 2013) the possibility of the appearance of the μ-phase type $(Ni, Co)_7(Cr, W, Re, Mo)$ in W-, Mo-, and Cr-rich zones on the refractory alloys is demonstrated. It is possible to consider the formation of μ-phases of different compositions after the titanium–aluminum metallization on the nickel alloy investigated.

The (Ti, Zr)N layer, which divides zone II into two parts remains without destructions, pores, and cracks after the titanium–aluminum saturation. As a result of the chemical-thermal treatment it is dissolved in the (Ti, Zr)N layer into 1.8 wt.% Ni, 0.5 wt.% Cr, and 0.3 wt.% Al. The microanalysis proves the presence of Zr only in the (Ti, Zr)N layer, which confirms the stable existence of this compound in chemical-thermal treatment.

The concentration of titanium in the heterogeneous columnar crystals zone remained as previously at a level of 6.4 wt.%. At the same time, a substantial change in the concentration of Co, Al, Cr, Ni, Mo, and W in this case is caused by a different content of elements in light and dark parts of the coatings. The concentrations of Mo, W, and Cr in the NiAl layer at a distance of 1.5–2.0 μm from the zone of columnar crystals are 0.3 wt.%, 1.0 wt.%, and 6.2 wt.%, respectively (regime 2). The concentration of the same elements in the white columnar crystals achieves 36.8 wt.%,

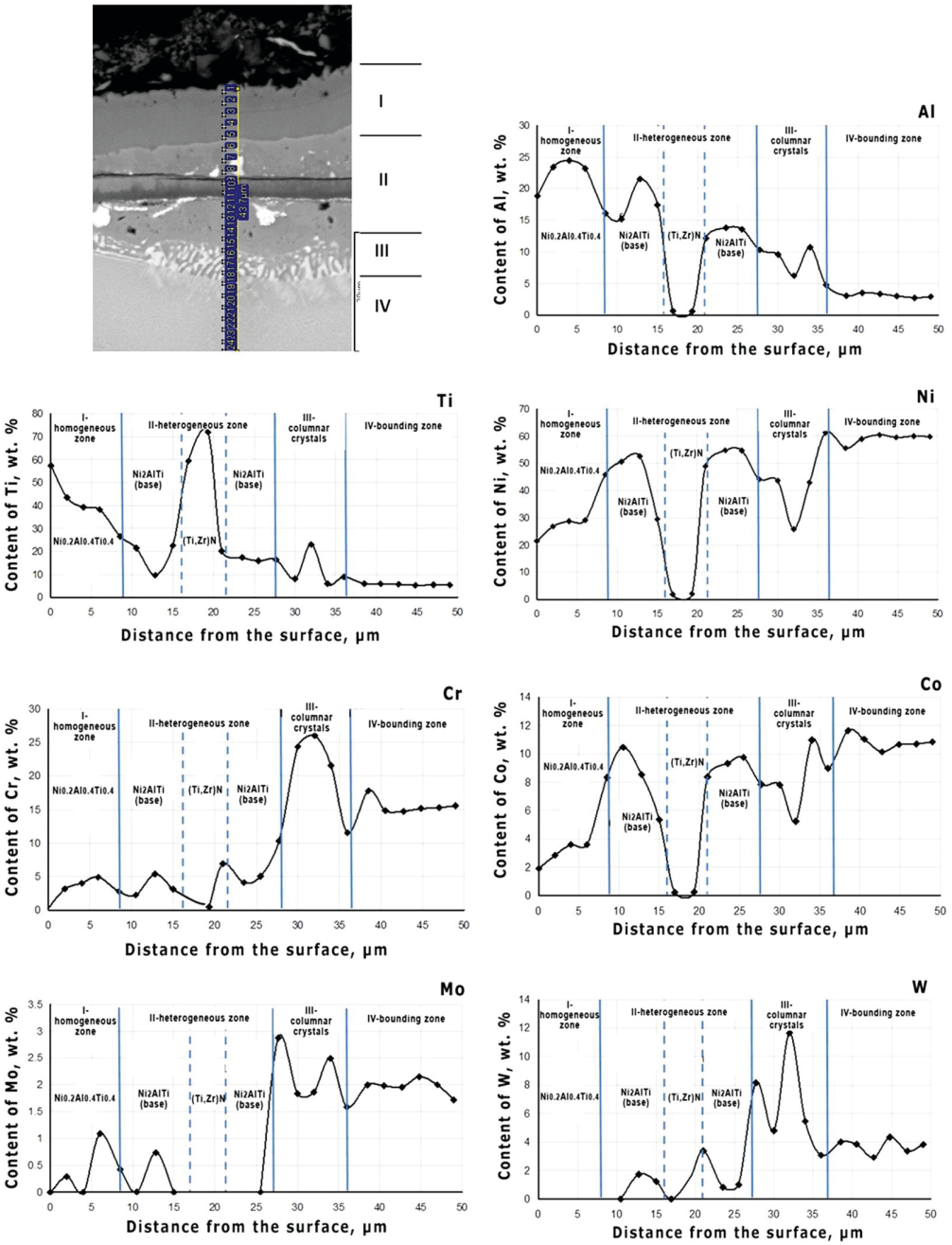

FIG. 4: Distribution of chemical elements over the thickness of titanium–aluminum coatings on the NiCrCoTiAlWMo alloy; regime 3

6.5 wt.%, and 20.1 wt.%, respectively, and falls in the direction of the border with a substrate.

Directly under the layer of columnar crystals, a layer of gray and dark-gray crystals with well-defined, almost a straight border with the previous zone, is situated. The crystallographic bonds between the grains of both layers are evident in the continuing dark and light grains of the columnar zone, the shape, sizes, and grain's morphology of the boundary zone.

The microhardness of separate intermetallic layers, heterogeneous structures on the basis of the coatings phases obtained range from 2.4 to 15.3 GPa. The microhardness of the (Ti, Zr)N layer after the titanium–aluminum saturation increased from 20.5 GPa to 22.1 GPa due to the alloying of the nitride phases with aluminum and nickel. The microhardness of the bounding zone is somewhat different from the microhardness of the substrate, and its values are affected by the regime of the chemical-thermal treatment. Under the layer of columnar crystals, the microhardness of the bounding zone is 4.0–4.3 GPa, and it reduces to the value of the substrate of 3.0–3.1 GPa.

4. CONCLUSIONS

In the present work, the possibility of the formation of HEAs coatings on the surface of nickel alloy is shown by combining physical vapor deposition of nitride (Ti, Zr)N and diffusion titanium–aluminum metallization, which was conducted in a mixture of Ti, Al, Al_2O_3, and NH_4Cl powders.

It is found that the coatings obtained consist of the Ni_2AlTi, NiAl, and $Ni_{0.2}Al_{0.4}Ti_{0.4}$ (λ-phase) compounds, oxides, and the μ-phase. The presence of a barrier layer (Ti, Zr)N is accompanied by changes in the phase composition and in the structure of the titanium–aluminum coatings. Instead of small spherical μ-phase impurities of diameter 0.5–1.5 μm, large (2.5–15.0 μm) complicated-shape grains of the same phase are formed near the (Ti, Zr)N layer. The high entropy $Ni_{0.2}Al_{0.4}Ti_{0.4}$ (λ-phase) layer occurs as a result of the barrier layer with the interaction of saturation elements.

The microhardness of separate intermetallic layers, heterogeneous structures of the coatings after the titanium–aluminum saturation enhances from 2.4 to 15.3 GPa, when the microhardness of the (Ti, Zr)N layer increases negligibly up to 22.1 GPa.

The obtained titanium–aluminum coatings with the (Ti, Zr)N barrier layer on a nickel alloy by phase, chemical composition, and the structure can be promising in terms of the high temperatures and corrosive environment conditions.

Further studies will be directed at establishing the heat resistance, mechanical properties of the coatings produced, as well as at the improvement of the processing of chemical-thermal treatments.

REFERENCES

Braic, V., Vladescu, A., Balaceanu, M., Luculescu, C., and Braic, M., Nanostructured multi-element TiZrNbHfTaN and TiZrNbHfTaN hard coatings, *Surf. Coat. Technol*., vol. **211**, pp. 117–121, 2012.

Gorban, V.F., Shahinian, R.A., Krapivka, N.A., Firstov, S.A., Danilenko, N.I., and Serdyuk, I.V., Superhard vacuum-based coatings on the base of high entropy alloys, *J. Powder Metall.*, nos. 11–12, pp. 114–121, 2015.

Karpets, M.V., Myslyvchenko, O.M., Krapivko, M.O., Hunchback, V.F., Makarenko, O.S., and Nazarenko, V.A., Influence of plastic deformation on the phase composition, texture and mechanical properties of the high entropy alloy $CrMnFeCoNi_2Cu$, *J. Superhard Mater.,* vol. **1**, pp. 30–36, 2015.

Khyzhniak, V.G. and Arshuk, M.V., Diffusion coatings with titanium and aluminum on steel 12Kh18N10T, *Izv. Vyssh. Ucheb. Zaved., Chern. Metallur.*, vol. **5**, pp. 68–69, 2011.

Klopotov, V.D., Potekaev, A.I., Klopotov, A.A., Kulagina, V.V., Knestyapin, E.A., Markova, T.N., and Morozov, M.M., Ternary diagram on the base titanium aluminides. Analysis and structure, *Bull. Tomsk. Polytech. Univ.*, vol. **323**, no. 2, pp. 96–100, 2013.

Kolomytsev, P.T., *High-Temperature Protective Coatings for Nickel Alloys*, Moscow: Metallurgiya Press, pp. 82–150, 1991.

Krause-Rehberg, R., Pogrebnyak, A.D., Borisyuk, V.N., Kaverin, M.V., Ponomarev, A.G., Bilokur, M.A., Oyoshi, K., Takeda, Y., Beresnev, V.M., and Sobol', O.V., Analysis of local regions near interfaces in nanostructured multicomponent (Ti–Zr–Hf–V–Nb)N coatings produced by the cathodic-arc-vapor-deposition from an arc of an evaporating cathode, *Phys. Met. Metallogr.*, vol. **114**, no. 8, pp. 672–680, 2013.

Maboyadzhan, S.A., Lesnikov, V.P., and Kuznetsov, V.P., *Complex Protective Coatings of Turbine Blades of Aviation GTEs*, Ekaterinburg: Kvist Press, pp. 144–145, 2008.

Pogrebnjak, A.D., Bondar, O.V., Borba, S.O., Abadias, G., Konarski, P., Plotnikov, S.V., Beresnev, V.M., Kassenova, L.G., and Drodziel, P., Nanostructured multielement (TiHfZrNbVTa)N coatings before and after implantation of N+ ions (10^{18} cm^{-2}): Their structure and mechanical properties, *Nucl. Instrum. Meth. B*, vol. **385**, pp. 74–83, 2016a.

Pogrebnjak, A.D., Bor'ba, S.O., Kravchenko, Ya.O., Tleukenov, E.O., Plotnikov, C.V., Beresnev, V.M., Takeda, Y., Oyoshi, K., and Kupchishin, A.I., Effect of the high doze of N+ (10^{18} cm^{-2}) ions implantation into the (TiHfZrVNbTa)N nanostructured coating on its microstructure, elemental and phase compositions, and physico-mechanical properties, *J. Superhard Mater.*, vol. **38**, no. 6, pp. 393–401, 2016b.

Pogrebnyak, A.D., Baghdasaryan, A.A., Yakushchenko, I.V., and Beresnev, V. M., The structure and properties of high-entropy alloys and nitride coatings based on them, *Rus. Chem. Rev.*, vol. **83**, no. 11, pp. 1027–1061, 2014.

Schuster, I.C., Pan, Z., Liu, S., Weitzer, F., and Du, Y., On the constitution of the ternary system Al–Ni–Ti, *J. Intermetallics*, vol. **15**, pp. 1257–1267, 2007.

Tsai, D.C., Haung, Y.L., Lin, S.R., Liang, S.C., and Shieu, F.S., Effect of nitrogen blow rations on the structure and mechanical properties of (TiVCrZrY)N coatings prepared by reactive magnetron sputtering, *Appl. Surf. Sci*., vol. **257**, pp. 1361–1367, 2010.

Voroshnin, L.G., Mendeleeva, O.S., and Smetkin, V.A., *The Theory and Technology of Chemical-Thermal Treatment,* Moscow: Novoe Znanie Press, pp. 196–236, 2010.

Zhang, Y. and Zhou, Y.J., Solid solution formation criteria for high entropy alloys, *Mater. Sci. Forum*, vols. **561–565**, pp. 1337–1339, 2007.